Oncogene (2014), 1–12
© 2014 Macmillan Publishers Limited All rights reserved 0950-9232/14
www.nature.com/onc

ORIGINAL ARTICLE

The Parkinson's gene PINK1 regulates cell cycle progression and promotes cancer-associated phenotypes

CH O'Flanagan[1], VA Morais[2,3], W Wurst[4,5,6], B De Strooper[2,3,7] and C O'Neill[1]

PINK1 (phosphatase and tensin homolog deleted on chromosome 10 (PTEN)-induced kinase 1), a Parkinson's disease-associated gene, was identified originally because of its induction by the tumor-suppressor PTEN. PINK1 promotes cell survival and potentially metastatic functions and protects against cell stressors including chemotherapeutic agents. However, the mechanisms underlying PINK1 function in cancer cell biology are unclear. Here, using several model systems, we show that PINK1 deletion significantly reduced cancer-associated phenotypes including cell proliferation, colony formation and invasiveness, which were restored by human PINK1 overexpression. Results show that PINK1 deletion causes major defects in cell cycle progression in immortalized mouse embryonic fibroblasts (MEFs) from PINK1$^{-/-}$ mice, and in BE(2)-M17 cells stably transduced with short hairpin RNA against PINK1. Detailed cell cycle analyses of MEF cell lines from several PINK1$^{-/-}$ mice demonstrate an increased proportion of cells in G2/M and decreased number of cells in G1 following release from nocodazole block. This was concomitant with increased double and multi-nucleated cells, a reduced ability to undergo cytokinesis and to re-enter G1, and significant alterations in cell cycle markers, including failure to increase cyclin D1, all indicative of mitotic arrest. PINK1$^{-/-}$ cells also demonstrated ineffective cell cycle exit following serum deprivation. Cell cycle defects associated with PINK1 deficiency occur at points critical for cell division, growth and stress resistance in cancer cells were rescued by ectopic expression of human PINK1 and demonstrated PINK1 kinase dependence. The importance of PINK1 for cell cycle control is further supported by results showing that cell cycle deficits induced by PINK1 deletion were linked mechanistically to aberrant mitochondrial fission and its regulation by dynamin-related protein-1 (Drp1), known to be critical for progression of mitosis. Our data indicate that PINK1 has tumor-promoting properties and demonstrates a new function for PINK1 as a regulator of the cell cycle.

Oncogene advance online publication, 31 March 2014; doi:10.1038/onc.2014.81

INTRODUCTION

PINK1 (*phosphatase and tensin homolog deleted on chromosome 10 (PTEN)-induced kinase 1*) was first identified in HeLa cells as a gene upregulated by overexpression of the central tumor suppressor, PTEN.[1] Subsequently, loss of function mutations in *PINK1* were discovered to cause autosomal recessive Parkinson's disease,[2] and a wealth of research on PINK1 function in neuronal and other cell systems emerged.[3–8] The *PINK1* gene encodes a 581-amino-acid protein with a highly conserved serine/threonine kinase domain, a C-terminal auto-regulatory sequence and a mitochondrial-targeting signal.[9,10] PINK1 is ubiquitously expressed,[11] and is a major regulator of mitochondrial quality control, including bioenergetics and the triad of fission, fusion and mitophagy.[12–14] PINK1 also demonstrates significant cytoprotective and anti-apoptotic functions,[5,6,15,16] including via the phosphatidylinositol 3 kinase/Akt/mammalian target of rapamycin axis[17,18] proteasomal[19–21] and autophagic pathways.[22,23]

Many of the functions of PINK1 draw increasing attention to the importance of this kinase in regulation of cell survival systems outside those protecting from neurodegeneration in Parkinsonism. This is especially pertinent when considering cell survival in cancer, where a number of studies have indicated a potential role for PINK1 in tumorigenesis.[17,24–26] However, the mechanisms underlying PINK1 function in cancer biology are not clear and have been the subject of only a few investigations, with conflicting evidence as to whether PINK1 has tumor-promoting or -suppressive activity. When considering tumor promotion, PINK1 is necessary for optimal activation of insulin-like growth factor-1 receptor–phosphatidylinositol 3 kinase/Akt signaling, a well-described oncogenic pathway.[18] Moreover, PINK1-mediated activation of Akt via mammalian target of rapamycin complex 2 increases migration, a key feature of invasive cancer cells.[17] High-throughput RNA interference screens have identified PINK1 deletion as a primary sensitizer of chemoresistant cancer cells to cell death following treatment with paclitaxel[26] and as a target for treatment of malignancies with DNA mismatch repair deficiencies.[25] In the context of tumor suppression, PINK1 is induced by PTEN[1] and FOXO3a[27] tumor suppressors, and associates with Beclin-1, another tumor suppressor.[22] Parkin, an autosomal recessive Parkinson's disease-causing gene, can function downstream of PINK1 (reviewed in Jin and Youle[28] and Wilhelmus and Nijland[29]) and is also a tumor suppressor.[30–32] The *PINK1* gene is located on chromosome 1p36[1], a region postulated to contain tumor-suppressive activity.[33] Such opposing context-dependent pro- and antitumorigenic properties are emerging to be common for many genes with tumorigenic

[1]School of Biochemistry and Cell Biology, BioSciences Institute, University College Cork, Cork, Ireland; [2]VIB Center for the Biology of Disease, VIB, Leuven, Belgium; [3]Center for Human Genetics and LIND, KU Leuven, Leuven, Belgium; [4]Helmholtz Zentrum München, German Research Center for Environmental Health, Institute of Developmental Genetics, München-Neuherberg, Germany; [5]Technische Universität München-Weihenstephan, Lehrstuhl für Entwicklungsgenetik, c/o Helmholtz Zentrum München, München-Neuherberg, Germany; [6]German Center for Neurodegenerative Diseases (DZNE), Munich, Germany and [7]UCL Institute of Neurology, London, UK. Correspondence: Dr C O' Neill, School of Biochemistry and Cell Biology, BioSciences Institute, University College Cork, Cork IRL, Ireland.
E-mail: c.oneill@ucc.ie
Received 12 August 2013; revised 12 December 2013; accepted 12 January 2014

potential,[34,35] and it has been postulated that PINK1 may have a dual role, being either anti-apoptotic or anti-growth depending on cellular context.[24]

Many of the mitochondrial functions ascribed to PINK1 are centrally linked to regulation of cell death and survival in cancer cells. Mitochondrial fission is strongly associated with apoptosis[36,37] and mitochondrial DNA mutations, altered metabolic pathways, increased mitochondrial reactive oxygen species, and deregulated mitochondrial dynamics contribute to the development of malignant cells.[38–41] It is well documented that regulation of the fission/fusion axis via the mitochondrial fission GTPase dynamin-related protein-1 (Drp1) is a major function of PINK1 in *Drosophila*.[42–44] In dividing mammalian cells, PINK1 deletion causes excessive fission, and deletion of Drp1 can rescue the PINK1-null phenotype.[13,45] Importantly, the mitochondrial fission/fusion and bioenergetic balance is critical for cell cycle progression, cell division and growth, with fission being essential for equal distribution of mitochondria during mitosis,[46–48] whereas fused mitochondrial networks are important for progression from G1 to S phase[49] and stress resistance during starvation.[50,51]

Much evidence thus supports a function for PINK1 in cancer cell biology, although the underlying mechanism(s) are unclear. Therefore, this study aimed to investigate PINK1 function in cancer cell phenotypes. Our results show, for the first time, that PINK1 deletion causes cell cycle defects associated with aberrant regulation of mitochondrial fission, and highlight PINK1 as a regulator of the cell cycle and as a candidate oncogene.

RESULTS

PINK1 deletion suppresses several cancer-associated phenotypes

Initial experiments aimed to determine the impact of PINK1 deletion on tumor-associated phenotypes including cell proliferation, colony formation, migration and invasiveness (Figure 1). Cells with PINK1 deletion including several immortalized mouse embryonic fibroblast (MEF) lines derived from $n=3$ PINK1$^{-/-}$ mice, HeLa cells with stable knockdown of PINK1 and MCF-7 cells with transient knockdown of PINK1, all demonstrated significantly reduced proliferation rates compared with controls (Figure 1a). The slower growth rate of PINK1$^{-/-}$ compared with PINK1$^{+/+}$ MEFs, was rescued by overexpression of human *wild-type* PINK1 (hPINK1$_{res}$), but not by the triple kinase dead[52] PINK1 mutant (hPINK1$_{K219A/D362A/D384A}$) (Figure 1a). Colony formation assays revealed a significant decrease in clonogenic potential in PINK1$^{-/-}$ compared with PINK1$^{+/+}$ MEFs, which was restored in hPINK1$_{res}$ cells, but not by hPINK1$_{K219A/D362A/D384A}$ (Figure 1b). Reduced colony formation was also observed in HeLa cells with stable PINK1 knockdown (Figure 1c), although not in MCF-7 cells with transient PINK1 deletion via small interfering RNA (siRNA) (data not shown), most likely due to the transient nature of siRNA deletion. Though deletion of PINK1 did not alter cell migration in wound-healing assays of fibroblasts, overexpression of human PINK1 caused a significant increase in cell migration (Figure 1d), as was found also using transwell migration assays (data not shown). In addition, PINK1$^{-/-}$ cells were found to be less invasive than their PINK1$^{+/+}$ counterparts (Figure 1e), which was rescued in hPINK1$_{res}$ MEFs. Taken together, these results indicate that PINK1 is required for key cell phenotypes associated with cancer progression.

PINK1 deficiency alters cell cycle profile and increases the frequency of multi-nucleated cells

We were next interested to examine the mechanism by which PINK1 deletion reduced tumorigenic phenotypes. Here, we focused first on analysis of immortalized MEF cell lines derived from three pairs of PINK1$^{+/+}$ and PINK1$^{-/-}$ mice. Microscopic examination of these PINK1$^{-/-}$ MEFs revealed morphological differences compared with PINK1$^{+/+}$ MEFs, whereby PINK1$^{-/-}$ cells appeared larger and flatter, a description commonly used for senescent cells.[53] Use of a senescence assay to detect β-galactosidase activity (Figure 2a) and cell cycle analysis (Figure 2b) with late passage (p6) non-immortalized MEFs as a positive control showed only p6 MEFs were senescent, as shown by reduced cycling cells and increased cells in G0/G1.

However, these results did reveal significant differences in the cell cycle profile of PINK1$^{-/-}$ compared with PINK1$^{+/+}$ cells, whereby deletion of PINK1 caused a significant increase in the number of cells in G2/M phase, concomitant with a significant decrease in the percentage of cells in G0/G1 phases (Figure 2b). These changes were rescued by overexpression of human PINK1, although not rescued by the PINK1$_{K219A/D362A/D384A}$ mutant (Figure 2b). This observation was supported by morphological analysis of each of the three independently derived PINK1$^{-/-}$ MEF lines, which consistently revealed a highly significant increase in the frequency of double and multi-nucleated cells compared with PINK1$^{+/+}$ MEFs (Figure 2c). This phenotype was rescued in hPINK1$_{res}$ MEFs and significantly less effectively in hPINK1$_{K219A/D362A/D384A}$ MEFs. (Figure 2c). Results further showed that, similar to MEFs lacking PINK1, BE(2)-M17, a dopaminergic neuroblastoma cell line, stably transduced with short hairpin RNA (shRNA) sequences directed against PINK1[13] demonstrated a significant increase in the number of cells in G2/M phase, concomitant with a significant decrease in the percentage of cells in G0/G1 phases, compared with cells with control shRNA and the parental BE(2)-M17 line (Supplementary Figure 1).

Taken together, these results indicate that PINK1 deletion alters cell cycle profile, increasing both the number of cells in G2/M and multi-nucleated cells, a phenotype that would impact on effective cell division and growth, which is rescued by overexpression of PINK1 and involves PINK1 kinase activity.

PINK1 deletion impairs cell division during G2/M

Next, we performed a more stringent analyses of the impact of PINK1 deletion at G2/M phase following synchronization with the mitotic spindle inhibitor nocodazole. The percentage of cells in G2/M did not reduce over time in PINK1$^{-/-}$ MEFs following release from nocodazole block, as seen in PINK1$^{+/+}$ MEFs (Figure 3a, Supplementary Figure 2). Thus, PINK1$^{-/-}$ cells remained in G2/M phase up to 2 h post-nocodazole release (Figure 3a), which was rescued by overexpression of hPINK1. A high proportion of hPINK1$_{K219A/D362A/D384A}$ MEFs also remained in G2/M, but by 2 h, this population was reduced, although not to the same extent as PINK1$^{+/+}$ or hPINK1$_{res}$ MEFs.

The inability of PINK1-deficient cells to exit G2/M phase was also observed using double immunofluorescence with 4,6-diamidino-2-phenylindole and α-tubulin, which showed that the majority of PINK1$^{-/-}$ cells had not divided 2 h post-release from nocodazole block (Figure 3b). PINK1-deficient cells underwent chromosome segregation and nuclear envelope reformation, indicating that this defect occurs at cytokinesis. In contrast at this time point, PINK1$^{+/+}$, and hPINK1$_{res}$ cells had divided into two daughter cells associated only by the tubulin-rich midbody, indicative of the end stage of cytokinesis. hPINK1$_{K219A/D362A/D384A}$ MEFs showed both dividing cells and multi-nucleated cells, indicating only partial rescue of the cell division defect at this time point (Figure 3b). Together, these data indicate that the inability to progress from G2/M to G1 induced by PINK1 deficiency is rescued by human PINK1 and involves PINK1 kinase activity. Immunofluorescence microscopy revealed that human PINK1 localized to distinct poles at the periphery of the mitotic plane throughout mitosis and showed increased colocalization with the tubulin cytoskeleton at cytokinesis (Supplementary Figure 3).

Results further showed significant alterations in the profile of key cell cycle-associated proteins in PINK1$^{-/-}$ compared

© 2014 Macmillan Publishers Limited

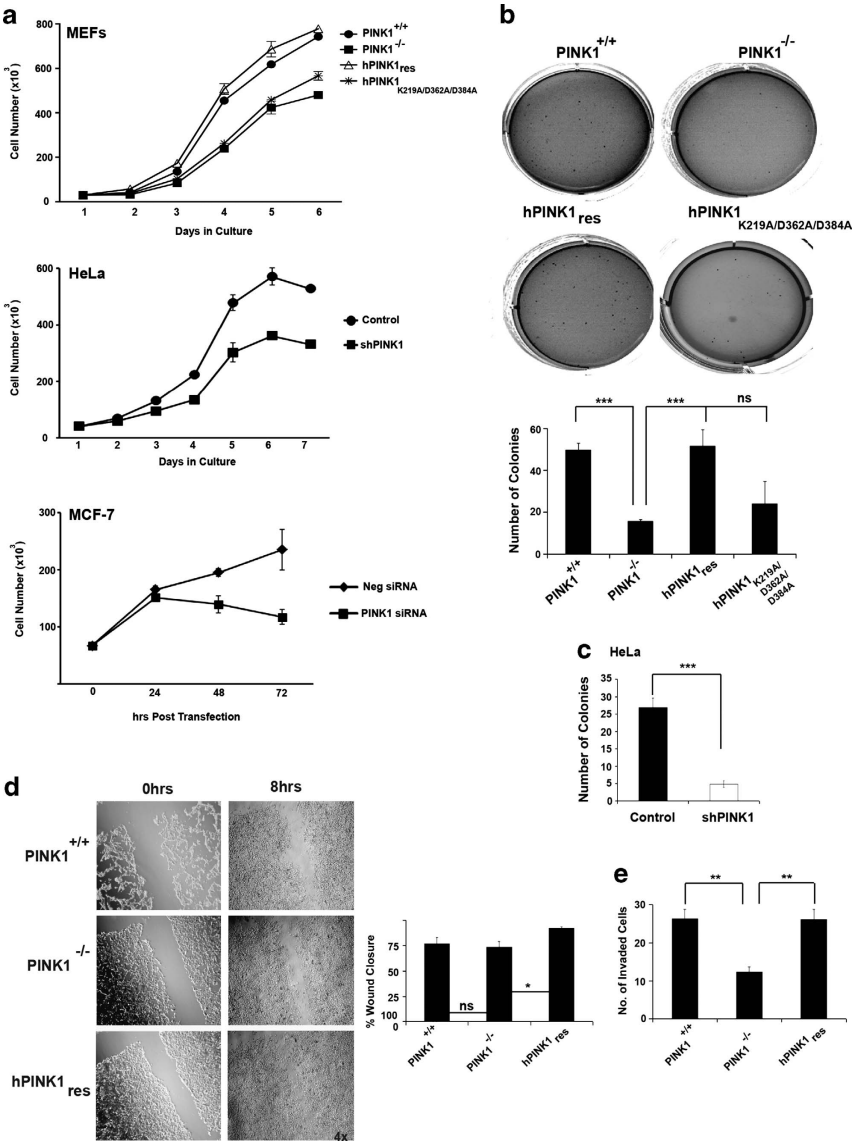

Figure 1. PINK1 deletion reduced cancer-causing phenotypes. (**a**) Growth rates of immortalized PINK1$^{+/+}$ (circles), PINK1$^{-/-}$ (squares), hPINK1$_{res}$ (triangles) and hPINK1$_{K219A/D362A/D384A}$ (asterisks) MEFs; HeLa (circles) and shPINK1 HeLa cells (squares); and MCF-7 cells transfected with negative control (diamonds) or PINK1 siRNA (squares). Cells were seeded at a density of 4×10^4 cells per well and growth was monitored every 24 h by cell counting. Curves are representative of mean ± s.e.m. of immortalized MEF cell lines derived from PINK1$^{+/+}$ ($n = 3$) and PINK1$^{-/-}$ ($n = 3$) mice. (**b**) Colony formation assays of PINK1$^{+/+}$, PINK1$^{-/-}$, hPINK1$_{res}$, hPINK1$_{K219A/D362A/384A}$ MEFs (**c**) control and shPINK1 HeLa cells. Cells were cultured in soft agarose for 14–21 days and resulting colonies were stained and counted. The graph in (**b**) and (**c**) shows the mean ± s.e.m. values for triplicate wells of three independent experiments. For MEFs and Hela cells, the number of colonies is significantly decreased by PINK1 deletion (***$P < 0.001$, Student's *t*-test). In MEFs, the colony number is significantly restored by hPINK1res rexpression (***$P < 0.001$, Student's *t*-test) but not so by the hPINK1$_{K219A/D362A/384A}$ mutant (ns, nonsignificant) (**d**) Scratch wound migration assay of PINK1$^{+/+}$, PINK1$^{-/-}$ and hPINK1$_{res}$ MEFs. Monolayers were scored and cells were allowed to migrate into the wound for 8 h. Graph shows quantification of the mean ± s.e.m. % wound closure of triplicate wells of a representative experiment (*$P < 0.05$, Student's *t*-test; ns, nonsignificant). (**e**) Invasion assay of PINK1$^{+/+}$, PINK1$^{-/-}$ and hPINK1$_{res}$ MEFs. Cells were deprived of serum and allowed to migrate into a matrigel-coated transwell chamber for 24 h toward media containing 10% serum. Invasive cells were stained and photographed on a light microscope. Graphs represent mean ± s.e.m. of triplicate wells from three independent experiments. (**$P < 0.01$, Student's *t*-test).

with PINK1$^{+/+}$ fibroblasts up to 24 h post-release from nocodazole block (Figure 3c), consistent with the altered cell cycle profile. Phospho-histone H3, which is phosphorylated early in mitosis, is not phosphorylated at 6 h or even up to 24 h following nocodazole release in PINK1$^{-/-}$ cells, as occurs in PINK1$^{+/+}$ MEFs, with partial rescue in hPINK1$_{res}$ cells, indicating that PINK1$^{-/-}$ cells do not undergo subsequent mitosis at the same rate as the control cells. Total histone H3 levels were not significantly different in PINK1$^{-/-}$, PINK1$^{+/+}$ or hPINK1$_{res}$ cells. Moreover, cyclin D1, whose increase in G1 phase is essential for cell cycle entry, is markedly reduced at all time points in PINK1$^{-/-}$ compared with PINK1$^{+/+}$ cells, with cyclin D1 expression levels restored toward wild-type levels in hPINK1$_{res}$ cells.

The mitotic kinase (MBP, mitotic-promoting factor) cyclin B1/Cdk1 is essential for initiation of the mitotic programme with reduction of cyclin B1 levels being necessary for mitotic exit.[46] Cyclin B1 and Cdk1 expression profiles are altered in PINK1$^{-/-}$ compared with PINK1$^{+/+}$ MEFs, with cyclin B1 failing to increase at later time points and increased Cdk1 expression at all time points in PINK1$^{-/-}$ MEFs (Figure 3c). Unlike cyclin D1 expression

© 2014 Macmillan Publishers Limited

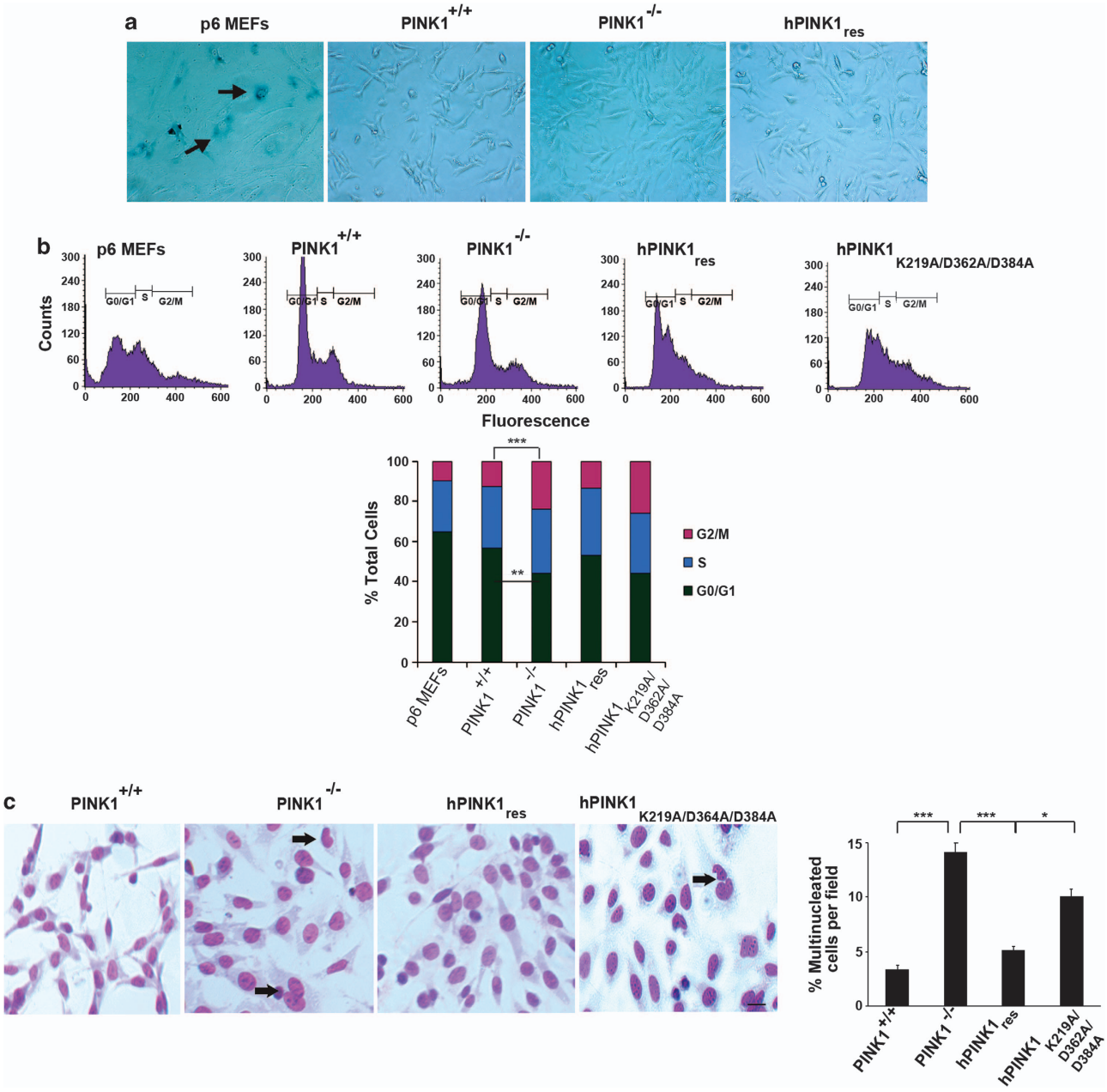

Figure 2. PINK1 deletion alters cell cycle profile and increases multi-nucleation. (**a**) Senescence assay for PINK1$^{+/+}$, PINK1$^{-/-}$ and hPINK1$_{res}$ MEFs, with late passage, non-immortalized p6 MEFs as positive control. Cells were fixed and stained with X-gal and imaged using a light microscope. Arrows indicate senescence-associated β-galactosidase activity occurs uniquely in p6 MEFS (blue staining). (**b**) Cell cycle analysis of PINK1$^{+/+}$, PINK1$^{-/-}$, hPINK1$_{res}$ and hPINK1$_{K219A/D362A/D384A}$ MEFs, as well as p6 non-immortalized MEFs showing representative flow cytometry analysis with histograms showing the average percentage of cells in G0/G1 (green), S (blue) and G2/M (pink) phases. Data shown represent mean ± s.e.m. of immortalized MEF cell lines derived from PINK1$^{+/+}$ ($n=3$) and PINK1$^{-/-}$ ($n=3$) mice (***$P<0.001$, **$P<0.01$, Student's *t*-test, when comparing G2/M and G0/G1, respectively, in PINK1$^{-/-}$ and PINK1$^{+/+}$ MEFs). hPINK1res but not hPINK1$_{K219A/D362A/D384A}$ restore G2/M and G0/G1 average percentages to PINK1$^{+/+}$ levels. (**c**) Morphological analysis of PINK1$^{+/+}$, PINK1$^{-/-}$, hPINK1$_{res}$ and hPINK1$_{K219A/D362A/D384A}$ MEFs. Arrows indicate multi-nucleation in representative PINK1$^{-/-}$ and in hPINK1$_{K219A/D362A/D384A}$ MEFs. Images were taken in 10 random fields from each of three coverslips per individual sample. Histograms represent the mean percentage ± s.e.m. of multi-nucleated cells per field of MEF cell lines derived from PINK1$^{+/+}$ ($n=3$) and PINK1$^{-/-}$ ($n=3$) mice (***$P<0.001$, *$P<0.05$, Student's *t*-test).

and histone H3 phosphorylation, these changes were not rescued in hPINK1$_{res}$ MEFs. p53 levels are similar up to 24 h post-release from nocodazole block in all cells. These results were also reflected in BE(2)-M17 cells transduced with the PINK1 shRNA, which showed significantly reduced cyclin D1 expression, and significantly increased phospho-histone H3 levels and Cdk1 expression compared with cells with control shRNA (Supplementary Figure 4a). Together, these data indicate that PINK1 promotes progression through mitosis and cytokinesis to G1.

Multi-nucleation in PINK1-deficient cells is associated with increased mitochondrial fission

PINK1 function is inextricably linked with the maintenance of effective mitochondrial dynamics. Mitochondrial fission/fusion transitions are critical for cell cycle progression especially through

© 2014 Macmillan Publishers Limited

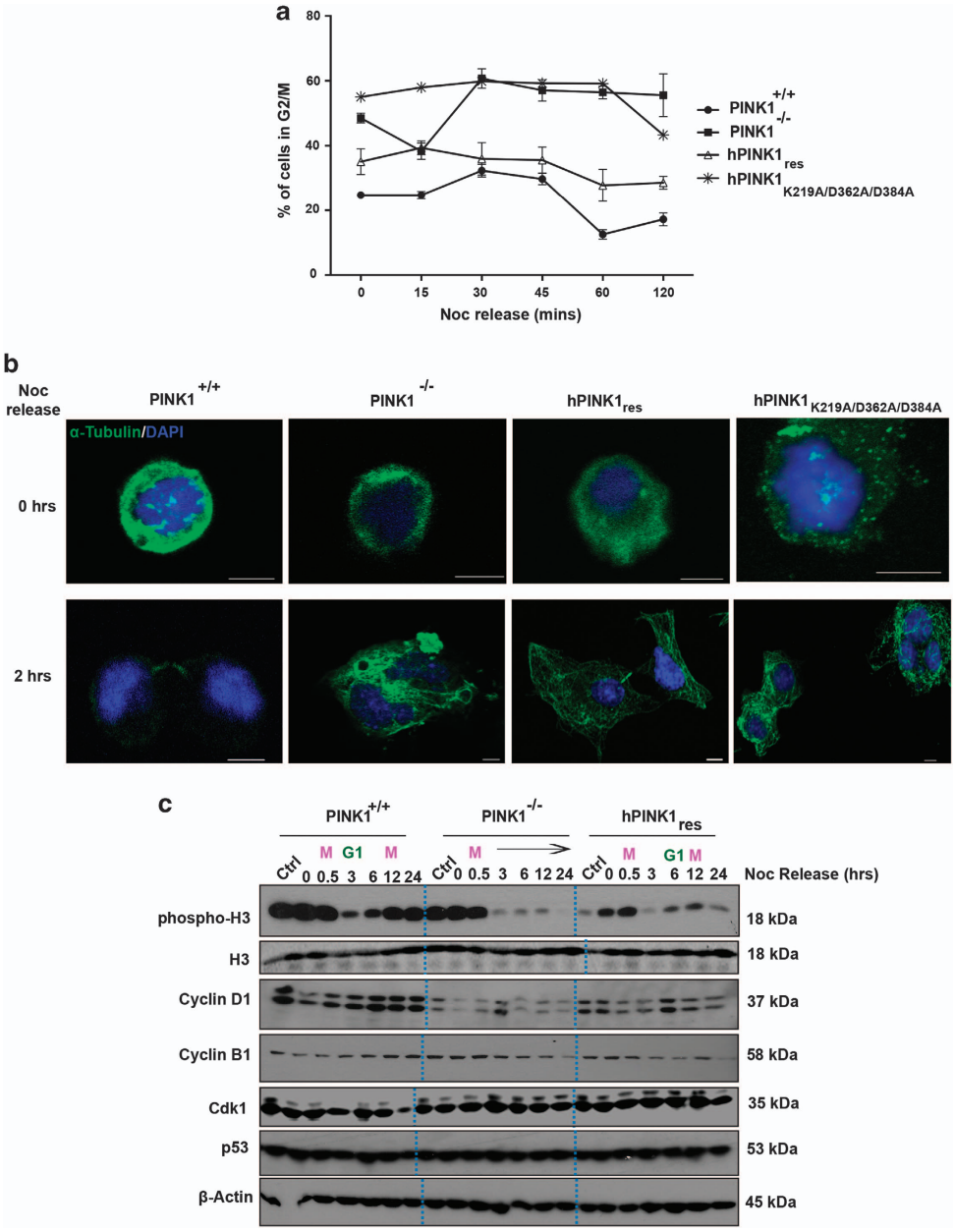

Figure 3. PINK1-deficient cells have impaired cell division. (**a**) Percentage of cells in G2/M phase of the cell cycle following release from mitotic block with nocodazole in PINK1$^{+/+}$ (circles) PINK1$^{-/-}$ (squares), hPINK1$_{res}$ (triangles) and hPINK1$_{K219A/D362A/D384A}$ (asterisks) MEFs. Cells were treated with 40 ng/ml nocodazole for 16 h, washed and cultured for the indicated times up to 120 min in complete culture media before being harvested for cell cycle analysis. PINK1$^{-/-}$ MEFs and hPINK1$_{K219A/D362A/D384A}$ have a sustained high percentage of cells in G2/M up to 120 min post-nocodazole block. Values are mean ± s.e.m. of triplicate samples from three independent experiments. (**b**) Confocal immunofluorescence microscopy of cells following mitotic release. MEFs were harvested by mitotic shake off, seeded onto coverslips and released from nocodazole block for 2 h before being fixed and stained with 4,6-diamidino-2-phenylindole (DAPI; blue) and α-tubulin (green) at both 0 and 2 h post-nocodazole release. Representative images of dividing cells were captured on a confocal microscope. After 2 h, PINK1$^{+/+}$ and hPINK1$_{res}$ MEFs have divided into daughter cells associated only by the tubulin-rich midbody at cytokinesis, PINK1$^{-/-}$ cells or hPINK1$_{K219A/D362A/D384A}$ have not undergone cytokinesis at this time point with multiple nuclei encapsulated in one cell cytoplasm. Scale bars 5 μm. (**c**) Representative immunoblot analysis showing relative expression of cell cycle-associated proteins in PINK1$^{+/+}$, PINK1$^{-/-}$ and hPINK1$_{res}$ MEFs, which were harvested at the indicated times up to 24 h post-release from nocodazole block. Predicted cell cycle phases (M and G1) are indicated above the immunoblot. Expression profiles of phospho-H3 and cyclin D1 are significantly altered, in PINK1$^{-/-}$ compared with PINK1$^{+/+}$ cells and are partially rescued by hPINK1$_{res}$.

G2/M to G1[47], although this has never been investigated in the context of PINK1. Mitochondrial fission during mitosis is essential for the equal distribution of mitochondria to daughter cells,[46] whereas inhibition of fission and transition to a fused state permits progression through cytokinesis to G1[47]. We thus hypothesized that the regulation of mitochondrial fission/fusion by PINK1 is important mechanistically in the transition to G1, and that defects in this regulation are an underlying mechanism in the failure of PINK1$^{-/-}$ cells to complete mitosis, leading to multi-nucleation.

Confocal microscopy revealed a small but significant decrease in mitochondrial interconnectivity (Figure 4a) but not elongation

© 2014 Macmillan Publishers Limited

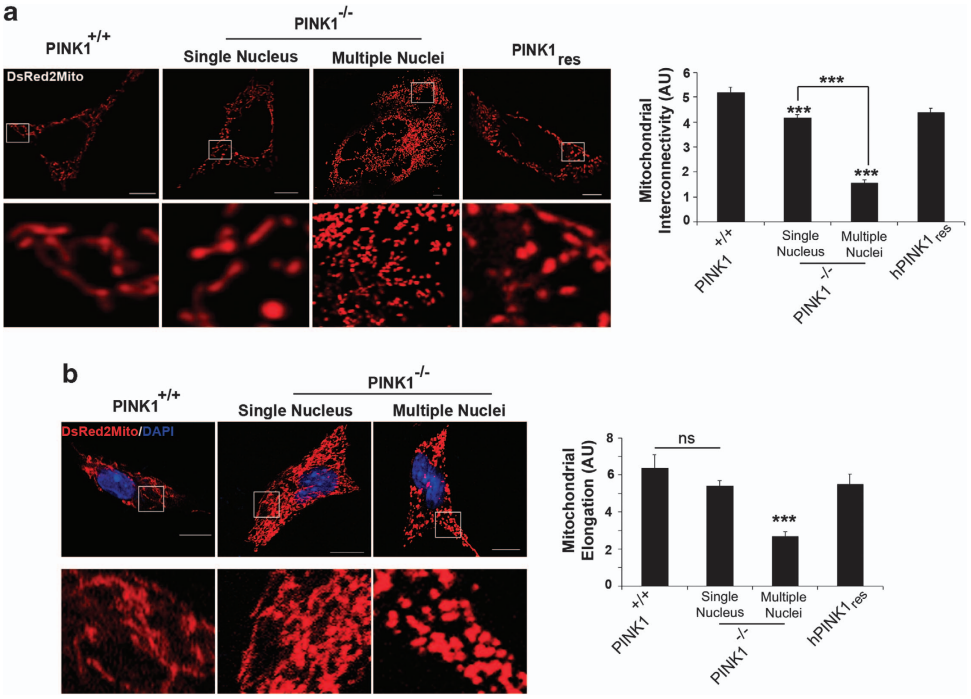

Figure 4. Multi-nucleation and G2/M block in PINK1$^{-/-}$ cells is associated with increased mitochondrial fission. Representative live cell (**a**) and fixed (**b**) confocal microscopy images showing mitochondrial morphology in PINK1$^{+/+}$, PINK1$^{-/-}$, multi-nucleated PINK1$^{-/-}$ and hPINK1$_{res}$ MEFs. Cells were transfected with pDsRed2-Mito for 12 h before being photographed. Fixed cells were permeabilized and stained with 4,6-diamidino-2-phenylindole (DAPI; blue). Scale bars 5 μm. Graphs show quantification of mitochondrial interconnectivity and elongation (***$P < 0.001$, analysis of variance with Tukey's post-test; ns, nonsignificant).

(Figure 4a), both measures of mitochondrial fusion,[54] in single nucleated PINK1$^{-/-}$ MEFs compared with PINK1$^{+/+}$ cells. Importantly, however, PINK1$^{-/-}$ cells that exhibited multi-nucleation were found to have a highly significant decrease in both mitochondrial interconnectivity and elongation, indicating major mitochondrial fragmentation and fission in cells which fail to divide (Figure 4a). Exogenous expression of hPINK1 rescues this fission and hPINK1$_{res}$ cells demonstrated significantly increased levels of mitochondrial interconnectivity and elongation compared with PINK1$^{-/-}$ multi-nucleated cells (Figure 4a). Similar results were observed when cells were fixed and stained with the nuclear stain 4,6-diamidino-2-phenylindole to identify multiple nuclei (Figure 4b).

PINK1-deficiency induced G2/M defects associate with impaired Drp1 regulation

The GTPase Drp1 is the major mediator of mitochondrial fission, and Drp1 function has been linked to PINK1 previously,[13,45] albeit never in the context of cell cycle progression where Drp1 function is critical.[46,47,55] During mitosis, Drp1 expression, mitochondrial recruitment and activity increase inducing mitochondrial fission. Mitochondria are distributed to daughter cells in metaphase, and Drp1 expression and activity decreases subsequently in anaphase and cytokinesis, through degradation via the anaphase-promoting complex (APC/C^{cdh1}),[48] as mitochondria return to a more fused morphology.[46,55,56]

Therefore, we investigated whether impaired regulation of Drp1 is associated with the cell cycle defects caused by PINK1 deficiency. Immunoblot analysis showed Drp1 expression was significantly higher in PINK1$^{-/-}$ (Figure 5a) compared with PINK1$^{+/+}$ MEFs, which was restored by overexpression of human PINK1, but less effectively in cells expressing the kinase dead hPINK1$_{K219A/D362A/D384A}$ or partial kinase dead hPINK1$_{K219A}$ mutants.[52] Double immunofluorescence of Drp1 and MitoTracker Green (MTG) showed Drp1 colocalized more strongly with mitochondria in PINK1$^{-/-}$ compared with PINK1$^{+/+}$ fibroblasts, which was most evident in cells that fail to divide and exhibit multi-nucleation (Figure 5b). Similarly, PINK1$^{-/-}$ cells overexpressing hPINK1$_{K219A/D362A/D384A}$ demonstrated increased Drp1/MitoTracker Green colocalization only in their multi-nucleated cells. Overexpression of hPINK1 rescued Drp1 cytoplasmic localization (Figure 5b).

Phosphorylation of Drp1 at Ser^{585} rat sequence (Ser^{616} human Drp1 variant 1) by cyclin B1/Cdk1 is essential for mitotic entry and for increased Drp1-mediated mitochondrial fission during metaphase neccessary for mitochondrial distribution to daughter cells at cytokinesis.[46,47] Thereafter, APC/C^{cdh1}-induced degradation of cyclin B1 coincides with reduced phospho-Drp1^{Ser585} levels, and increased Drp1 degradation essential for mitotic exit and increased mitochondrial fusion necessary for entry to G1.[46,47] We found that this phosphorylation-induced regulation of Drp1 during mitosis is impaired in PINK1$^{-/-}$ compared with PINK1$^{+/+}$ cells. Upon release from nocodazole block, Drp1 and phospho-Drp1^{Ser585} levels reduced slightly at 3 h in PINK1$^{+/+}$ cells during G1 phase. Thereafter, both Drp1 expression and phospho-Drp1^{Ser585} levels increased at 6 h, as the cells initiate the next round of mitosis and phospho-Drp1^{Ser585} levels migrate predominantly as a distinctive higher molecular weight band (Figure 5c). In stark contrast, Drp1 and phospho-Drp1^{Ser585} levels were significantly higher at time zero and all subsequent time points following release from nocodazole block in PINK1-deficient cells, where phospho-Drp1^{Ser585} is only evident as the higher molecular weight phosphorylated band at all time points (Figure 5c). This is indicative of sustained phosphorylation at Drp1^{Ser585} concomitant with prolonged residence in the mitotic pre-cytokinesis phase in PINK1$^{-/-}$ cells. Together, these results indicate that the multi-nucleation and failure to exit mitosis caused by PINK1 deficiency is linked to excessive mitochondrial fission, increased Drp1 expression, increased and sustained phosphorylation of Drp1^{Ser585}, and

© 2014 Macmillan Publishers Limited

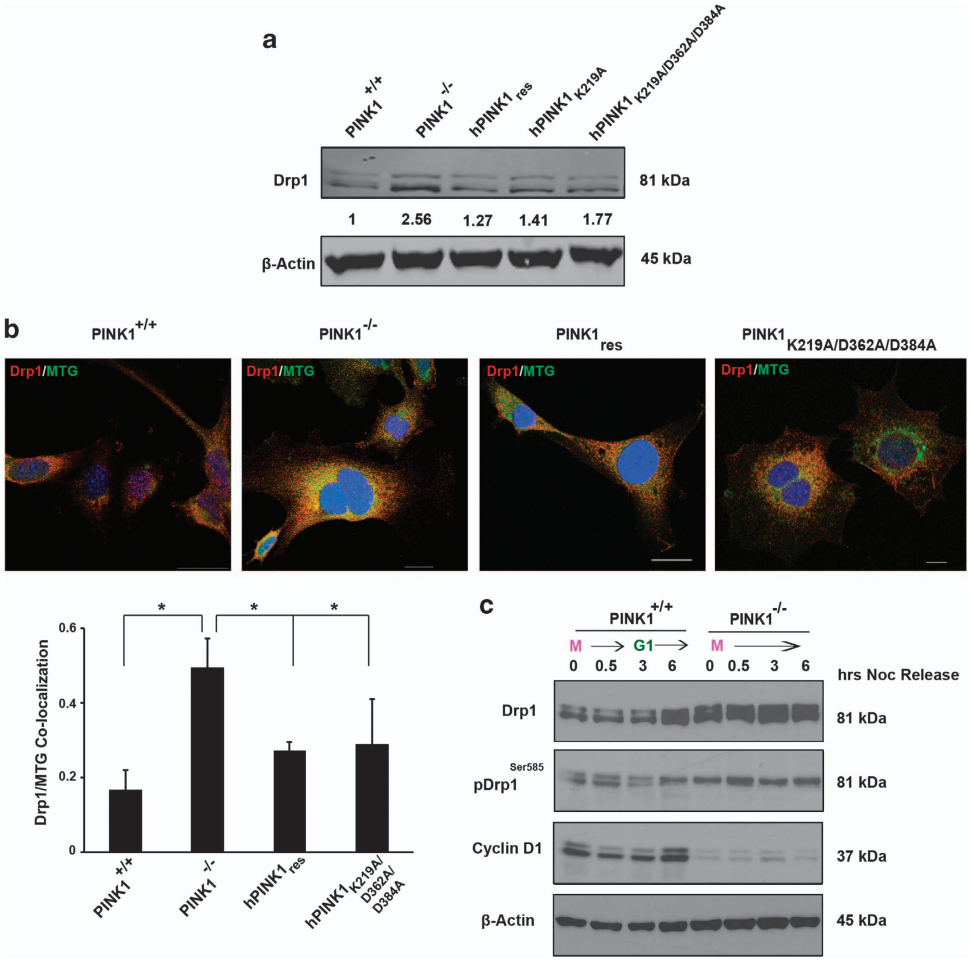

Figure 5. (**a**) Representative immunoblot showing Drp1 expression in PINK1$^{+/+}$, PINK1$^{-/-}$, hPINK1$_{res}$ and hPINK1$_{K219A/D362A/D384A}$ MEFs. Drp1 expression is increased in PINK1$^{-/-}$ cells, which is rescued by overexpression of human PINK1 and partially rescued by overexpression of the kinase impaired (K219A) and kinase dead (K219A/D362A/D384A) mutants. (**b**) Representative double immunofluorescence microscopy showing Drp1 (red) and MitoTracker green (MTG, green) colocalization with nuclei stained with 4,6-diamidino-2-phenylindole (DAPI; blue) in PINK1$^{+/+}$, PINK1$^{-/-}$ hPINK1$_{res}$ and hPINK1$_{K219A/D362A/D384A}$ MEFs. Increased Drp1 and MTG colocalization is evident in PINK1$^{-/-}$ cells with both double and single nuclei (middle panel) and more pronounced in cells with double nuclei. hPINK1$_{K219A/D362A/D384A}$ MEFs show increased Drp1/MTG colocalisation, which is selective to multi-nucleated cells. Histograms show mean colocalization values ± s.e.m. of Drp1 and MTG, which is significantly increased in PINK1$^{-/-}$ compared to PINK1$^{+/+}$ and is significantly reduced by overexpression of human PINK1 and by overexpression of hPINK1$_{K219A/D362A/D384A}$. (*$P < 0.05$, Student's *t*-test). Scale bars 10 μm. (**c**) Representative western immunoblots showing comparative Drp1, Drp1^{Ser585} phosphorylation and cyclin D1 protein levels in PINK1$^{+/+}$ and PINK1$^{-/-}$ MEFs at various time points up to 6 h post-nocodazole release. Drp1 and pDrp1^{Ser585} are significantly increased and have different time-dependent profiles in PINK1$^{-/-}$ compared with PINK1$^{+/+}$ cells, and cyclin D1 levels are significantly reduced at every time point in PINK1$^{-/-}$ cells.

increased Drp1 mitochondrial localization. As Drp1^{Ser585} is phosphorylated by cyclin B1/Cdk1, we sought to determine whether cyclin B1/Cdk1 complexes were increased in PINK1$^{-/-}$ compared with PINK1$^{+/+}$ fibroblasts. Cyclin B1 levels that co-immunoprecipitated with Cdk1 in PINK1$^{-/-}$ cells were marginally higher than in PINK1$^{+/+}$ cells (Supplementary Figure 4b). Together with the higher Cdk1 levels in PINK1$^{-/-}$ cells, this could tentatively indicate increased activity of the complex.

Knockdown of Drp1 reduces multi-nucleation caused by PINK1 deletion

In order to further investigate the effect of mitochondrial fission on cell cycle defects in PINK1-deficient cells, we used an RNA interference approach to suppress Drp1 expression in PINK1$^{-/-}$ MEFs. Transfection with Drp1 siRNA resulted in a decrease of ~50% of Drp1 protein expression in PINK1$^{-/-}$ MEFs (Figure 6a, lane 3) reducing Drp1 levels to the level found in PINK1$^{+/+}$ cells (Figure 6a, final lane). This resulted in reduced levels of fragmented mitochondria with increased levels of tubulated, interconnected mitochondria in PINK1$^{-/-}$ MEFs (Figure 6b), the characteristic morphology described previously following Drp1 knockdown.[46] Morphological analysis further showed that Drp1 knockdown significantly reduced the frequency of multi-nucleated cells in PINK1$^{-/-}$ MEFs (Figure 6c). Thus, inhibition of mitochondrial fission, via reduction of Drp1, rescues multi-nucleation caused by PINK1 deficiency.

G0/G1 cell cycle exit impairment in PINK1-deficient cells is also associated with defective mitochondrial dynamics

A significant decrease in the number of cells in G0/G1 phases was detected in PINK1-deficient MEFs (Figure 2b). To investigate this more stringently, cells were synchronized at G0/G1 by removal of growth factors for 24 h, with subsequent release into serum and cell cycle analysis (Figure 7a, Supplementary Figure 5). Serum deprivation causes cells to exit the cell cycle at G0/G1 and to stop dividing, as occurred in PINK1$^{+/+}$ fibroblasts (Figure 7a).

© 2014 Macmillan Publishers Limited

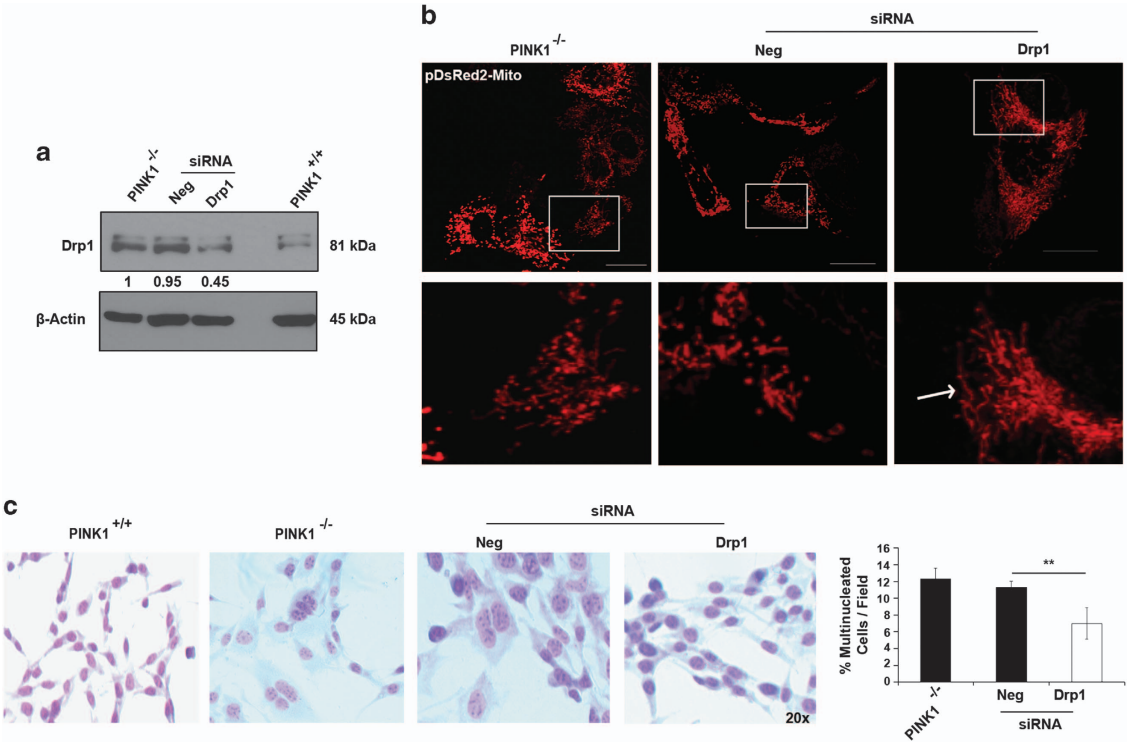

Figure 6. Inhibition of Drp1 reduces multi-nucleation caused by PINK1 deficiency. (**a**) Immunoblot analysis confirming Drp1 siRNA knockdown in PINK1$^{-/-}$ MEFs. Cells were transfected with siRNA for 24 h before being harvested for immunoblot analysis. PINK1$^{+/+}$ MEFs are included as an internal control (final lane). (**b**) Confocal microscopy showing mitochondrial morphology in pDsRed2-Mito-transfected PINK1$^{-/-}$ MEFs, MEFs transfected with Drp1 siRNA and negative control siRNA. Images show a mixture of fragmented and tubulated mitochondria in both PINK1$^{-/-}$ and PINK1$^{-/-}$ cells transfected with negative control siRNA. Mitochondrial fragmentation is reduced in PINK1$^{-/-}$ cells transfected with Drp1 siRNA where cells show the characteristic morphology of fused mitochondria, indicated by the arrow. Scale bars 10 μm. (**c**) Morphological analysis and quantification of multi-nucleated cells in PINK1$^{-/-}$ MEFs transfected with Drp1 or negative control siRNA. Cells were grown on coverslips, fixed and stained with Rapi Diff II and imaged using a light microscope. Multi-nucleated cells are evident in both PINK1$^{-/-}$ and PINK1$^{-/-}$ cells transfected with negative control siRNA, but not in PINK1$^{-/-}$ cells transfected with Drp1 siRNA. Graph represents the mean percentage of multi-nucleated cells per field ± s.e.m. of 10 random fields for each of three independent experiments. Drp1 deletion in PINK1$^{-/-}$ MEFs, but not negative control siRNA, significantly reduced the number of cells with multiple nuclei. Values are mean ± s.e.m. (**$P < 0.01$, analysis of variance with Tukey's post-test).

In contrast, significantly fewer PINK1$^{-/-}$ cells arrested in G0/G1, with 10% of cells remaining in G2/M. This was partially rescued in hPINK1$_{res}$, but not in hPINK1$_{K219A}$ MEFs, indicating PINK1 kinase dependence, for effective cell cycle exit. Upon restoration of serum, all cells re-entered the cell cycle, returning to their normal profile after 24 h (Supplementary Figure 5).

Reduced mitochondrial fission and increased mitochondrial membrane potential ($\Delta\psi_m$) have a protective role during serum deprivation-induced cell cycle exit.[50,51] Flow cytometry analysis with the potentiometric dye tetramethylrhodamine, ethyl ester showed that $\Delta\psi_m$ was significantly reduced in PINK1$^{-/-}$ compared with PINK1$^{+/+}$ fibroblasts (Figure 7b), as previously reported.[14] Moreover, we found that PINK1$^{-/-}$ MEFs did not undergo an increase in $\Delta\psi_m$ following serum deprivation as observed in PINK1$^{+/+}$ cells (Figure 7b). Serum deprivation caused no change to mitochondrial morphology in PINK1$^{+/+}$ MEFs, with a mix of both interconnected mitochondrial networks and punctate, circular mitochondria observed (Figure 7c). In contrast, removal of serum in PINK1$^{-/-}$ MEFs caused a striking induction of punctate, fragmented mitochondria, which was in part prevented by overexpression of hPINK1 (Figure 7c).

Double immunofluorescence microscopy of Drp1 with pDsRed2-Mito corroborated these findings and showed increased mitochondrially localized Drp1 upon serum deprivation in PINK1$^{-/-}$ MEFs compared with PINK1$^{+/+}$ cells (Figure 7d). A small percentage of mitotic cells were observed in PINK1$^{-/-}$ MEFs following 24-h incubation without growth factors supporting the cell cycle analysis (Figure 7d, bottom panel, 4,6-diamidino-2-phenylindole staining). These findings indicate that ineffective cell cycle exit caused by the absence of PINK1 is associated with increased Drp1-mediated mitochondrial fission and an inability to increase $\Delta\psi_m$ following serum deprivation. Taken together, our data indicate PINK1 regulates the cell cycle at stages critical for division, growth and stress resistance via regulation of mitochondrial function.

DISCUSSION

The past decade has seen substantial research into PINK1 function since its discovery as an autosomal recessive Parkinson's disease-causing gene. Recently, increasing attention has implicated PINK1 in a number of processes linked to cancer,[1,17,18,24–26] although limited information is available regarding fundamental mechanisms for PINK1 in cancer. This study demonstrates a new role for PINK1 as a cell cycle regulator at key points necessary for division, growth and stress resistance in cancer, and reveals that deletion of PINK1 inhibits several cancer-causing phenotypes including proliferation, colony formation and migration. Results show PINK1 kinase activity is necessary for proper cell cycle progression at G2/M specifically during cytokinesis, and during cell cycle exit at G0/G1. Although several reports have described varied roles for PINK1 in processes associated with cell cycle regulation, such as mitochondrial dynamics,[13,42,45] calcium flux,[13,57–59] phosphatidylinositol 3 kinase/Akt signaling[17,18] and autophagy,[28] this is the

© 2014 Macmillan Publishers Limited

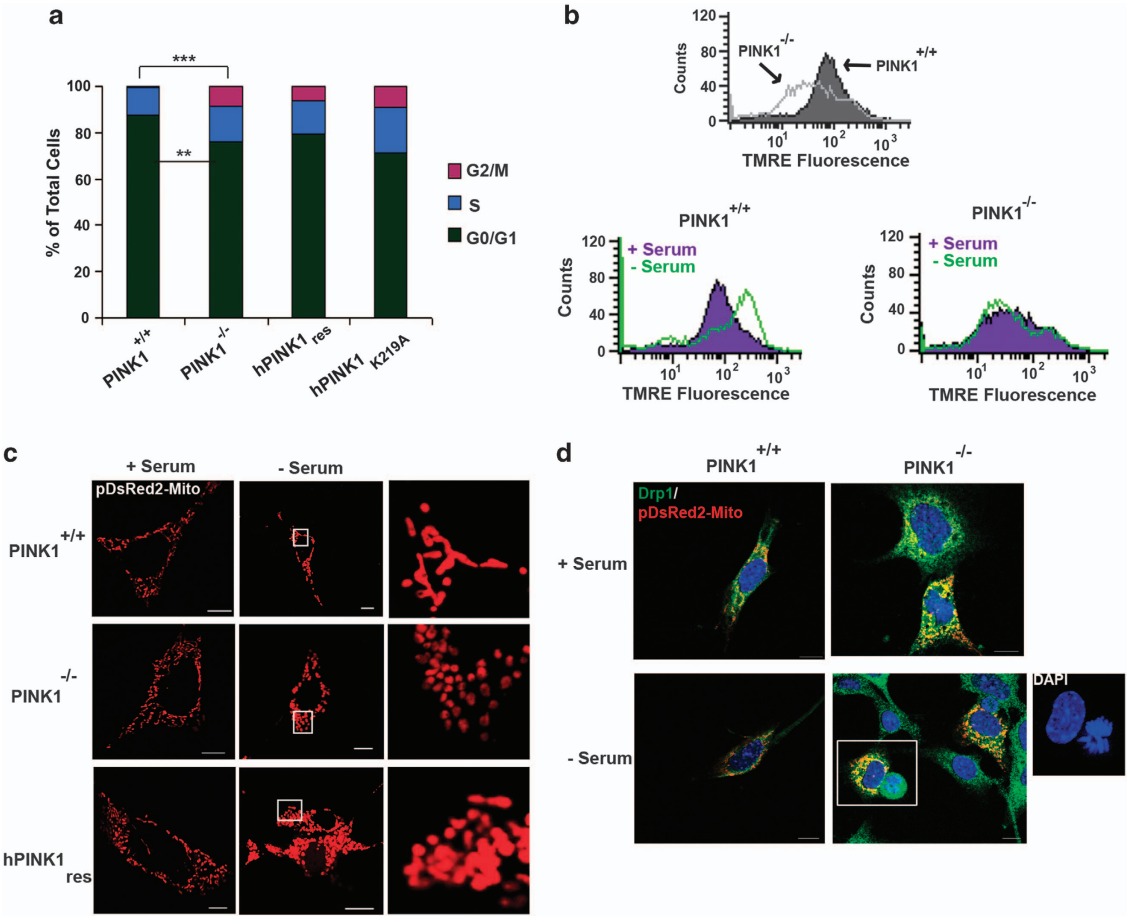

Figure 7. G0/G1 cell cycle exit impairment in PINK1$^{-/-}$ cells is linked to increased mitochondrial fission and an inability to increase $\Delta\psi_m$. (**a**) Cell cycle analysis of G0/G1 synchronized PINK1$^{+/+}$, PINK1$^{-/-}$, hPINK1$_{res}$ and hPINK1$_{K219A}$ MEFs. Cells were incubated with serum-free media for 24 h before being harvested for cell cycle analysis. (***$P < 0.001$, **$P < 0.01$, Student's *t*-test, when comparing G2/M and G0/G1, respectively, in PINK1$^{-/-}$ and PINK1$^{+/+}$ MEFs). (**b**) Fluorescence-activated cell sorting (FACS) analysis showing reduced $\Delta\psi_m$ in PINK1$^{-/-}$ (overlay) MEFs compared with PINK1$^{+/+}$ MEFs. Cells were stained with 50 nM tetramethylrhodamine, ethyl ester (TMRE) before being harvested for flow cytometry. PINK1$^{-/-}$ MEFs do not undergo an increase in $\Delta\psi_m$ upon removal of serum, as observed in PINK1$^{+/+}$ MEFs. At 24 h before flow cytometry, cells were incubated with or without serum. Graphs are representative of three independent experiments. (**c**) Representative confocal microscopy images showing PINK1$^{-/-}$ MEFs undergo increased levels of mitochondrial fission upon removal of serum compared with PINK1$^{+/+}$ and hPINK1res MEFs. pDsRed2-Mito-transfected PINK1$^{+/+}$, PINK1$^{-/-}$ and hPINK1res MEFs were incubated with and without serum for 24 h. Images are representative of four independent experiments. Scale bars 5 μm. (**d**) Confocal immunofluorescence microscopy showing Drp1 (green) colocalization with pDsRed2-Mito-transfected (red) in PINK1$^{+/+}$ and PINK1$^{-/-}$ MEFs incubated with and without serum for 24 h. DNA is stained with 4,6-diamidino-2-phenylindole (DAPI; blue). PINK1$^{-/-}$ MEFs have increased colocalization of Drp1 in mitochondria compared with PINK1$^{+/+}$ both with and without serum. Bottom right panel shows a cell in anaphase in serum starved PINK1$^{-/-}$ MEFs substantiating failed cell cycle exit. Scale bars 10 μm.

first study to directly implicate PINK1 in cell cycle control. These findings provide a potential mechanism, which could underlie several phenotypes previously described for PINK1 deficiency, and in the context of this study are of critical importance for cancer cell biology.

We also show that the regulation of Drp1-mediated mitochondrial fission is important in the control of cell cycle progression by PINK1 to transition from G2/M to G1 and to exit the cell cycle following serum deprivation. It is well documented that PINK1 regulates mitochondrial fission/fusion balance via Drp1[13,42–45], although this was not previously considered in the context of the cell cycle. Previous results, as also demonstrated here, showed that deletion of PINK1 in dividing cells causes excessive fission, rescued by Drp1 deletion.[13,45] In direct contrast, in terminally differentiated tissues in *Drosophila*, Drp1 overexpression rescues PINK1-null phenotypes.[43,44,60] This conundrum could be explained by our findings when considering the context-dependent regulation of Drp1 at different cell cycle stages in dividing cells and in terminally differentiated post-mitotic cells. Mitochondrial fission/fusion and bioenergetics are emerging to be critical for effective cell cycle progression.[46,47,49,55,56] Our findings now draw attention to the importance of further understanding the mitochondrial functions of PINK1 in cell cycle regulation in the context of both cancer and neurodegeneration.

Induction and completion of mitosis is essential for cancer cell proliferation, and much of the cell cycle machinery is increased in cancer cells.[61] Indeed, cyclin D1, found here to be reduced in PINK1-deficient cells, is a major proto-oncogene and driver of cell cycle progression.[62] PINK1 inhibition was shown previously to sensitize breast cancer cells to chemotherapeutic treatment with paclitaxel,[26] implicating PINK1 in chemoresistance. Paclitaxel inhibits spindle disassembly, causing cell death in dividing cells.[63] Here we show that deletion of PINK1 alone can prevent cell division, indicating a potential mechanism through which PINK1 inhibition and treatment with paclitaxel synergistically kills cancer cells, and lending further credence to PINK1 as a potential target in chemoresistant tumors. Impaired mitosis in PINK1-deficient cells will constrain proliferation and likely result in death,

© 2014 Macmillan Publishers Limited

however, failure to properly complete cell division and aneuploidy are feature of cancer cells.[64] Thus, in certain contexts, PINK1 deletion may facilitate gain of chromosomes, increasing the frequency of chromosomal aberrations and explain the opposing functions described for PINK1 in cancer.[24]

Cell cycle aberrations have primary functions in cancer but are also implicated in neurodegenerative disorders, where abortive cell cycle re-entry is mechanistically linked to cell death of post-mitotic neurons.[65–68] Thus, these results have clear importance for understanding PINK1 with respect to cell cycle regulation in cancer, but also when considering the protective function of PINK1 against neurodegeneration in Parkinson's disease.

MATERIALS AND METHODS

Generation of PINK1$^{-/-}$ mice and derived MEF cell lines

PINK1$^{-/-}$ knockout and *PINK1*$^{+/-}$ heterozygous knockout mice were generated by Wolfgang Wurst and Daniela Vogt-Weisenhorn (Helmholtz Center, Munich, Germany) and immortalized MEFs were generated as previously described.[14] Immortalized MEFs from three pairs of *PINK1*$^{-/-}$ and matched *PINK1*$^{+/+}$ mice were generated. In brief, *PINK1*$^{+/-}$ mice were interbred to generate mutant mice and wild-type littermate controls. Embryonic day 13 embryos were dissected, heads and red organs removed and used for genotyping. The rest of the bodies were chopped up in cell culture dishes containing Dulbecco's modified Eagle's medium supplied with 50% fetal bovine serum and 1% penicillin/streptomycin. Cultures were expanded and serum decreased to 10% fetal bovine serum after the attainment of consistent growth. Afterward cultures were immortalized by transfection with simian virus 40 (SV40) large T-antigen. *PINK1*$^{-/-}$ MEFs were stably transfected with a plasmid containing human PINK1 (hPINK1 construct Origene (Rockville, MD, USA)), the partial kinase dead hPINK1$_{K219A}$ and triple kinase dead hPINK1$_{K219A/D362A/D384A}$ mutants using site-directed mutagenesis (Stratagene, Santa Clara, CA, USA). hPINK1 expression was confirmed using RNA extraction and analysis. As indicated, experiments were performed using MEF lines from three pairs of *PINK1*$^{+/+}$ and *PINK1*$^{-/-}$ mice.

Cell culture and cell synchronization

MEFs, MCF-7 and HeLa cells were cultured in dulbecco's modified eagle's medium supplemented with 10% fetal bovine serum and 2 mM L-glutamine in a humidified atmosphere containing 5% CO_2 at 37 °C. BE (2)-M17 cells transduced with PINK1 shRNA or with control shRNA were kindly provided by Mark Cookson and Alexandra Beilina NIA, Bethesda, MD, USA and were transduced and cultured as previously described.[13] G2/M synchronization was achieved by treatment with 40 ng/ml nocodazole in complete media for 16 h. Cells were synchronized at G0/G1 phase by incubation with serum-free dulbecco's modified eagle's medium for 24 h.

Plasmids, siRNA and shRNA transfection

MEFs were transfected with pDsMitoRed2-Mito (Clontech, Palo Alto, CA, USA) using Lipofectamine 2000 (Invitrogen, Carlsbad, CA, USA) according to the manufacturer's instructions and incubated with DNA/Lipofectamine transfection mix for at least 12 h before being imaged on a Zeiss LSM 510 META Confocal microscope (Jena, Germany) or being fixed for immunofluorescence. For siRNA knockdown, MCF-7 cells or PINK1$^{-/-}$ MEFs were transfected for 24–48 h with 100 nM negative control siRNA (Ambion, Austin, TX, USA), PINK1-targeting siRNA (Qiagen, Germantown, MD, USA) or Drp1-targeting siRNA (Sigma, St Louis, MO, USA) using HiPerfect (Qiagen) according to the manufacturer's instructions. Stable PINK1 knockdown was achieved in HeLa cells using a 29mer shRNA construct against human PINK1 cloned into a retroviral untagged vector (Origene). The shRNA sequence was 5′-CCAGAACCTGGAGGTGACAAAGAGCACCG-3′. Cells were transfected with Lipofectamine 2000 and selected with 5 μg/ml puromycin.

Proliferation and colony formation assays

Cells were seeded at 4×10^4 cells per well in a 24-well plate. To monitor cell growth at intervals, attached cells were removed from quadruplicate wells using trypsin-ethylenediaminetetra acetic acid and viable cells counted by Trypan blue exclusion. Anchorage-independent cell growth was determined by assaying colony formation in soft agarose as described previously.[69] In all, 1×10^3 cells were resuspended in 0.33% low-melting point agarose (Sigma) in dulbecco's modified eagle's medium/10% fetal bovine serum and plated in triplicate onto 35-mm dishes containing a 2-ml base agarose layer (0.6%). After 14 days, colonies were stained with 0.01% crystal violet in 20% ethanol and counted.

Migration and invasion assays

Cells were plated in triplicate in six-well plates. Confluent monolayers were scratched using a sterile tip (time 0 h) and cells were allowed to migrate into the wound for 8 h. Wound closure was determined comparing the same field at 0 and 8 h using T-Scratch software.[70] For invasion assays, 1×10^5 cells were allowed to migrate into a 5 μM pore Transwell, pre-coated with 7 mg/ml Matrigel (BD Biosciences, Heidelberg, Germany). After 24 h, cells were fixed with 100% methanol, stained with 0.1% crystal violet and counted using a light microscope.

Cell cycle analysis and flow cytometry

For cell cycle analysis, cells were resuspended in ice-cold phosphate-buffered saline. Before flow cytometry, NP-40 and propidium iodide (Sigma) were added at a final concentration of 0.1% and 50 μg/ml, respectively. DNA content was measured in the FL2 channel using CellQuest software (Becton Dickinson, Oxford, UK). $\Delta\psi_m$ was measured by incubation with 50 nM tetramethylrhodamine, ethyl ester (Molecular Probes, Eugene, OR, USA) before being harvested for flow cytometry, with $\Delta\psi_m$ measured in the FL2 channel.

Confocal microscopy and morphological analysis

Fluorescence images were acquired Zeiss LSM 510 META confocal microscope fitted with a 63×/1.4 plan apochromat lens (Jena, Germany). For details of confocal microscopy and morphological analysis, see Supplementary Materials and methods.

Western blot analysis

Proteins were extracted for sodium dodecyl sulfate–polyacrylamide gel electrophoresis and western immunoblot analysis was performed as described in Supplementary Materials and methods.

CONFLICT OF INTEREST

The authors declare no conflict of interest.

ACKNOWLEDGEMENTS

We are grateful to Mark Cookson and Alexandra Beilina, National Institute on Aging, Bethesda, MD, USA for providing us with BE(2)-M17 cells transduced with control and PINK1 shRNA. We thank Rosemary O'Connor, School of Biochemistry and Cell Biology, University College Cork (UCC) for many helpful discussions, Sandra Yeomans UCC for technical assistance and Daniela Vogt-Weisenhorn, Helmholtz Centrum München, for helpful input. This work was funded by the Health Research Board of Ireland, PhD Scholars' Programme in Cancer Biology. Support from Science Foundation Ireland (SFI) (RFP), the FWO Foundation for Scientific Research Belgium, a Methusalem grant of the Flemish Government and the KU Leuven, and the Helmholtz Alliance for Mental Health in an Ageing Society is also gratefully acknowledged. BDS is the Arthur Bax and Anna Vanluffelen Chair for Alzheimer's disease. The Molecular Cell Biology group, UCC, provided access to a Zeiss 510 Confocal microscope, funded by an SFI Programme Grant to Mary W McCaffrey.

REFERENCES

1 Unoki M, Nakamura Y. Growth-suppressive effects of BPOZ and EGR2, two genes involved in the PTEN signaling pathway. *Oncogene* 2001; **20**: 4457–4465.
2 Valente EM, Abou-Sleiman PM, Caputo V, Muqit MMK, Harvey K, Gispert S *et al.* Hereditary early-onset Parkinson's disease caused by mutations in PINK1. *Science* 2004; **304**: 1158–1160.
3 Dodson MW, Guo M. Pink1, Parkin, DJ-1 and mitochondrial dysfunction in Parkinson's disease. *Curr Opin Neurobiol* 2007; **17**: 331–337.
4 Gispert S, Ricciardi F, Kurz A, Azizov M, Hoepken H-H, Becker D *et al.* Parkinson phenotype in aged PINK1-deficient mice is accompanied by progressive mitochondrial dysfunction in absence of neurodegeneration. *PloS One* 2009; **4**: e5777.

© 2014 Macmillan Publishers Limited

5 Haque ME, Thomas KJ, D'Souza C, Callaghan S, Kitada T, Slack RS *et al.* Cytoplasmic Pink1 activity protects neurons from dopaminergic neurotoxin MPTP. *Proc Natl Acad Sci USA* 2008; **105**: 1716–1721.
6 Petit A, Kawarai T, Paitel E, Sanjo N, Maj M, Scheid M *et al.* Wild-type PINK1 prevents basal and induced neuronal apoptosis, a protective effect abrogated by Parkinson disease-related mutations. *J Biol Chem* 2005; **280**: 34025–34032.
7 Kitada T, Pisani A, Porter DR, Yamaguchi H, Tscherter A, Martella G *et al.* Impaired dopamine release and synaptic plasticity in the striatum of PINK1-deficient mice. *Proc Natl Acad Sci USA* 2007; **104**: 11441–11446.
8 Wang H-L, Chou A-H, Yeh T-H, Li AH, Chen Y-L, Kuo Y-L *et al.* PINK1 mutants associated with recessive Parkinson's disease are defective in inhibiting mitochondrial release of cytochrome c. *Neurobiol Dis* 2007; **28**: 216–226.
9 Silvestri L, Caputo V, Bellacchio E, Atorino L, Dallapiccola B, Valente EM *et al.* Mitochondrial import and enzymatic activity of PINK1 mutants associated to recessive parkinsonism. *Human Mol Genet* 2005; **14**: 3477–3492.
10 Cardona F, Sánchez-Mut JV, Dopazo H, Pérez-Tur J. Phylogenetic and in silico structural analysis of the Parkinson disease-related kinase PINK1. *Hum Mutat* 2011; **32**: 369–378.
11 Gandhi S, Muqit MMK, Stanyer L, Healy DG, Abou-Sleiman PM, Hargreaves I *et al.* PINK1 protein in normal human brain and Parkinson's disease. *Brain* 2006; **129**: 1720–1731.
12 Liu W, Acín-Peréz R, Geghman KD, Manfredi G, Lu B, Li C. Pink1 regulates the oxidative phosphorylation machinery via mitochondrial fission. *Proc Natl Acad Sci USA* 2011; **108**: 12920–12924.
13 Sandebring A, Thomas KJ, Beilina A, Van der Brug M, Cleland MM, Ahmad R *et al.* Mitochondrial alterations in PINK1 deficient cells are influenced by calcineurin-dependent dephosphorylation of dynamin-related protein 1. *PLoS One* 2009; **4**: e5701.
14 Morais VA, Verstreken P, Roethig A, Smet J, Snellinx A, Vanbrabant M *et al.* Parkinson's disease mutations in PINK1 result in decreased Complex I activity and deficient synaptic function. *EMBO Mol Med* 2009; **1**: 99–111.
15 Pridgeon JW, Olzmann Ja, Chin L-S, Li L. PINK1 protects against oxidative stress by phosphorylating mitochondrial chaperone TRAP1. *PLoS Biol* 2007; **5**: e172.
16 Arena G, Gelmetti V, Torosantucci L, Vignone D, Lamorte G, De Rosa P *et al.* PINK1 protects against cell death induced by mitochondrial depolarization, by phosphorylating Bcl-xL and impairing its pro-apoptotic cleavage. *Cell Death Differ* 2013; **20**: 920–930.
17 Murata H, Sakaguchi M, Jin Y, Sakaguchi Y, Futami J, Yamada H *et al.* A new cytosolic pathway from a Parkinson disease-associated kinase, BRPK/PINK1: activation of AKT via mTORC2. *J Biol Chem* 2011; **286**: 7182–7189.
18 Akundi RS, Zhi L, Büeler H. PINK1 enhances insulin-like growth factor-1-dependent Akt signaling and protection against apoptosis. *Neurobiol Dis* 2012; **45**: 469–478.
19 Rakovic A, Grünewald A, Kottwitz J, Brüggemann N, Pramstaller PP, Lohmann K *et al.* Mutations in PINK1 and Parkin impair ubiquitination of mitofusins in human fibroblasts. *PLoS One* 2011; **6**: e16746.
20 Klinkenberg M, Thurow N, Gispert S, Ricciardi F, Eich F, Prehn JHM *et al.* Enhanced vulnerability of PARK6 patient skin fibroblasts to apoptosis induced by proteasomal stress. *Neuroscience* 2010; **166**: 422–434.
21 Muqit MMK, Abou-Sleiman PM, Saurin AT, Harvey K, Gandhi S, Deas E *et al.* Altered cleavage and localization of PINK1 to aggresomes in the presence of proteasomal stress. *J Neurochem* 2006; **98**: 156–169.
22 Michiorri S, Gelmetti V, Giarda E, Lombardi F, Romano F, Marongiu R *et al.* The Parkinson-associated protein PINK1 interacts with Beclin1 and promotes autophagy. *Cell Death Differ* 2010; **17**: 962–974.
23 Kawajiri S, Saiki S, Sato S, Sato F, Hatano T, Eguchi H *et al.* PINK1 is recruited to mitochondria with parkin and associates with LC3 in mitophagy. *FEBS Lett* 2010; **584**: 1073–1079.
24 Berthier A, Navarro S, Jiménez-Sáinz J, Roglá I, Ripoll F, Cervera J *et al.* PINK1 displays tissue-specific subcellular location and regulates apoptosis and cell growth in breast cancer cells. *Human Pathol* 2011; **42**: 75–87.
25 Martin SA, Hewish M, Sims D, Lord CJ, Ashworth A. Parallel high-throughput RNA interference screens identify PINK1 as a potential therapeutic target for the treatment of DNA mismatch repair-deficient cancers. *Cancer Res* 2011; **71**: 1836–1848.
26 MacKeigan JP, Murphy LO, Blenis J. Sensitized RNAi screen of human kinases and phosphatases identifies new regulators of apoptosis and chemoresistance. *Nat Cell Biol* 2005; **7**: 591–600.
27 Mei Y, Zhang Y, Yamamoto K, Xie W, Mak TW, You H. FOXO3a-dependent regulation of Pink1 (Park6) mediates survival signaling in response to cytokine deprivation. *Proc Natl Acad Sci USA* 2009; **106**: 5153–5158.
28 Jin SM, Youle RJ. PINK1- and Parkin-mediated mitophagy at a glance. *J Cell Sci* 2012; **125**: 795–799.
29 Wilhelmus M, Nijland P. Involvement and interplay of Parkin, PINK1 and DJ1 in neurodegenerative and neuroinflammatory disorders. *Free Radic Biol Med* 2012; **53**: 983–992.
30 Fujiwara M, Marusawa H, Wang H-Q, Iwai a, Ikeuchi K, Imai Y *et al.* Parkin as a tumor suppressor gene for hepatocellular carcinoma. *Oncogene* 2008; **27**: 6002–6011.
31 Veeriah S, Taylor BS, Meng S, Fang F, Yilmaz E, Vivanco I *et al.* Somatic mutations of the Parkinson's disease-associated gene PARK2 in glioblastoma and other human malignancies. *Nat Genet* 2010; **42**: 77–82.
32 Sun X, Liu M, Hao J, Li D, Luo Y, Wang X *et al.* Parkin deficiency contributes to pancreatic tumorigenesis by inducing spindle multipolarity and misorientation. *Cell Cycle* 2013; **12**: 1133–1141.
33 Bagchi A, Mills AA. The quest for the 1p36 tumor suppressor. *Cancer Res* 2008; **68**: 2551–2256.
34 Bernard D, Monte D, Vandenbunder B, Abbadie C. The c-Rel transcription factor can both induce and inhibit apoptosis in the same cells via the upregulation of MnSOD. *Oncogene* 2002; **21**: 4392–4402.
35 Chaiwatanasirikul KA, Sala A. The tumour-suppressive function of CLU is explained by its localisation and interaction with HSP60. *Cell Death Dis* 2011; **2**: e219.
36 Youle RJ, Karbowski M. Mitochondrial fission in apoptosis. *Nat Rev Mol Cell Biol* 2005; **6**: 657–663.
37 Youle RJ, Van der Bliek AM. Mitochondrial fission, fusion, and stress. *Science* 2012; **337**: 1062–1065.
38 Chatterjee A, Mambo E, Sidransky D. Mitochondrial DNA mutations in human cancer. *Oncogene* 2006; **25**: 4663–4674.
39 Grandemange S, Herzig S, Martinou J-C. Mitochondrial dynamics and cancer. *Semin Cancer Biol* 2009; **19**: 50–56.
40 Favre C, Zhdanov a, Leahy M, Papkovsky D, O'Connor R. Mitochondrial pyrimidine nucleotide carrier (PNC1) regulates mitochondrial biogenesis and the invasive phenotype of cancer cells. *Oncogene* 2010; **29**: 3964–3976.
41 Barbosa IA, Machado NG, Skildum AJ, Scott PM, Oliveira PJ. Mitochondrial remodeling in cancer metabolism and survival: Potential for new therapies. *Biochim Biophy Acta* 2012; **1826**: 238–254.
42 Poole AC, Thomas RE, Andrews LA, McBride HM, Whitworth AJ, Pallanck LJ. The PINK1/Parkin pathway regulates mitochondrial morphology. *Proc Natl Acad Sci USA* 2008; **105**: 1638–1643.
43 Deng H, Dodson MW, Huang H, Guo M. The Parkinson's disease genes pink1 and parkin promote mitochondrial fission and/or inhibit fusion in Drosophila. *Proc Natl Acad Sci USA* 2008; **105**: 14503–14508.
44 Poole AC, Thomas RE, Yu S, Vincow ES, Pallanck L. The mitochondrial fusion-promoting factor mitofusin is a substrate of the PINK1/parkin pathway. *PLoS One* 2010; **5**: e10054.
45 Lutz AK, Exner N, Fett ME, Schlehe JS, Kloos K, Lämmermann K *et al.* Loss of parkin or PINK1 function increases Drp1-dependent mitochondrial fragmentation. *J Biol Chem* 2009; **284**: 22938–22951.
46 Taguchi N, Ishihara N, Jofuku A, Oka T, Mihara K. Mitotic phosphorylation of dynamin-related GTPase Drp1 participates in mitochondrial fission. *J Biol Chem* 2007; **282**: 11521–11529.
47 Kashatus DF, Lim K-H, Brady DC, Pershing NLK, Cox AD, Counter CM. RALA and RALBP1 regulate mitochondrial fission at mitosis. *Nature Cell Biol* 2011; **13**: 1108–1115.
48 Horn SR, Thomenius MJ, Johnson ES, Freel CD, Wu JQ, Coloff JL *et al.* Regulation of mitochondrial morphology by APC/CCdh1-mediated control of Drp1 stability. *Mol Biol Cell* 2011; **22**: 1207–1216.
49 Mitra K, Wunder C, Roysam B, Lin G, Lippincott-Schwartz J. A hyperfused mitochondrial state achieved at G1-S regulates cyclin E buildup and entry into S phase. *Proc Natl Acad Sci USA* 2009; **106**: 11960–11965.
50 Rambold AS, Kostelecky B, Elia N, Lippincott-Schwartz J. Tubular network formation protects mitochondria from autophagosomal degradation during nutrient starvation. *Proc Natl Acad Sci USA* 2011; **108**: 10190–10195.
51 Gomes LC, Di Benedetto G, Scorrano L. During autophagy mitochondria elongate, are spared from degradation and sustain cell viability. *Nat Cell Biol* 2011; **13**: 589–598.
52 Beilina A, Van Der Brug M, Ahmad R, Kesavapany S, Miller DW, Petsko G *et al.* Mutations in PTEN-induced putative kinase 1 associated with recessive parkinsonism have differential effects on protein stability. *Proc Natl Acad Sci USA* 2005; **102**: 5703–5708.
53 Cho K, Ryu SJ, Oh YS, Park JH, Lee JW, Kim H-P *et al.* Morphological adjustment of senescent cells by modulating caveolin-1 status. *J Biol Chem* 2004; **279**: 42270–42278.
54 Dagda RK, Cherra SJ, Kulich SM, Tandon A, Park D, Chu CT. Loss of PINK1 function promotes mitophagy through effects on oxidative stress and mitochondrial fission. *J Biol Chem* 2009; **284**: 13843–13855.
55 Smirnova E, Griparic L, Shurland DL, Van der Bliek a M. Dynamin-related protein Drp1 is required for mitochondrial division in mammalian cells. *Mol Biol Cell* 2001; **12**: 2245–2256.
56 Yamano K, Youle RJ. Coupling mitochondrial and cell division. *Nat Cell Biol* 2011; **13**(9): 1026–1027.

© 2014 Macmillan Publishers Limited

57 Marongiu R, Spencer B, Crews L, Adame A, Patrick C, Trejo M *et al*. Mutant Pink1 induces mitochondrial dysfunction in a neuronal cell model of Parkinson's disease by disturbing calcium flux. *J Neurochem* 2009; **108**: 1561–1574.
58 Heeman B, Van den Haute C, Aelvoet S-A, Valsecchi F, Rodenburg RJ, Reumers V *et al*. Depletion of PINK1 affects mitochondrial metabolism, calcium homeostasis and energy maintenance. *J Cell Sci* 2011; **124**: 1115–1125.
59 Akundi RS, Huang Z, Eason J, Pandya JD, Zhi L, Cass WA *et al*. Increased mitochondrial calcium sensitivity and abnormal expression of innate immunity genes precede dopaminergic defects in Pink1-deficient mice. *PLoS One* 2011; **6**: e16038.
60 Park J, Lee G, Chung J. The PINK1-Parkin pathway is involved in the regulation of mitochondrial remodeling process. *Biochem Biophys Res Comm* 2009; **378**: 518–523.
61 Hanahan D, Weinberg RA. Hallmarks of cancer: the next generation. *Cell* 2011; **144**: 646–674.
62 Knudsen KE, Diehl JA, Haiman CA, Knudsen ES. Cyclin D1: polymorphism, aberrant splicing and cancer risk. *Oncogene* 2006; **25**: 1620–1628.
63 Bharadwaj R, Yu H. The spindle checkpoint, aneuploidy, and cancer. *Oncogene* 2004; **23**: 2016–2027.
64 Burgess DJ. Aneuploidy stokes the fire. *Nat Rev Cancer* 2011; **11**: 692.
65 Bonda DJ, Bajić VP, Spremo-Potparevic B, Casadesus G, Zhu X, Smith M a *et al*. Review: cell cycle aberrations and neurodegeneration. *Neuropathol Appl Neurobiol* 2010; **36**: 157–163.
66 Herrup K. The involvement of cell cycle events in the pathogenesis of Alzheimer's disease. *Alzheimers Res Ther* 2010; **2**: 13.
67 Herrup K, Yang Y. Cell cycle regulation in the postmitotic neuron: oxymoron or new biology? *Nat Rev Neurosci* 2007; **8**: 368–378.
68 Staropoli JF. Tumorigenesis and neurodegeneration: two sides of the same coin? *BioEssays* 2008; **30**: 719–727.
69 Ayllón V, O'connor R. PBK/TOPK promotes tumour cell proliferation through p38 MAPK activity and regulation of the DNA damage response. *Oncogene* 2007; **26**: 3451–3461.
70 Liang C-C, Park AY, Guan J-L. In vitro scratch assay: a convenient and inexpensive method for analysis of cell migration in vitro. *Nat Protoc* 2007; **2**: 329–333.

Supplementary Information accompanies this paper on the Oncogene website (http://www.nature.com/onc)

© 2014 Macmillan Publishers Limited